J. COMBIN. MATH. COMBIN. COMPUT. 125 (2025) 5187--5207

Journal of Combinatorial Mathematics and Combinatorial Computing
www.combinatorialpress.com/jcmcc

Optimization study of cable wiring scheme for photovoltaic power plant based on TS algorithm in the era of low-carbon development

Bin Ye[1], Xiang Li[2,✉], Yikun Cao[2]

[1] Zhejiang Qingneng Energy Development Corporation Limited, Zhejiang Provincial New Energy Investment Group Corporation Limited, Hangzhou, Zhejiang, 310007, China
[2] Chengdu Engineering Corporation Limited, Power China, Chengdu, Sichuan, 611130, China

ABSTRACT

As an important clean energy project, the optimization of the construction and operation of photovoltaic (PV) power plants is crucial in the context of the global active promotion of low-carbon development. This paper focuses on the optimization of cable wiring scheme for PV power plants based on the taboo search (TS) algorithm. A mathematical model is established by comprehensively considering the constraints such as power loss objective and tidal current calculation in the wiring optimization process. The wild dog optimization algorithm is improved using the Lévy flight algorithm, and the initialization phase of the taboo search algorithm is improved by the improved wild dog optimization algorithm, and the established cabling optimization model is solved using the improved taboo search algorithm (LDOA-TS). The experimental results show that the LDOA-TS algorithm has a significant performance advantage over other algorithms in the model solving process. At the same time, the simulation results obtained from the optimization model in this paper are basically consistent with the actual wiring pattern under different working conditions. And through the model of this paper for cable optimization wiring compared to the original wiring scheme in the point cable length and power loss were reduced by 30.30% and 49.95%, to meet the constraints at the same time to effectively achieve the model objectives, and has obvious economic benefits, in line with the needs of the low-carbon era of photovoltaic power plant construction and operation.

Keywords: forbidden search algorithm, Lévy flight algorithm, wild dog optimization algorithm, cable routing, photovoltaic power plant

✉ Corresponding author.
E-mail address: 18081900510@163.com (X. Li).
Received 25 February 2024; Revised 05 April 2024; Accepted 15 December 2024; Published Online 16 April 2025.
DOI: 10.61091/jcmcc127b-288

1. Introduction

Against the background of energy crisis and environmental degradation, countries around the world have taken the development and utilization of sustainable clean energy as their future development strategy, and the development trend of green and low-carbon energy centered on electricity has become more and more obvious [1-2]. Among them, solar energy is widely favored worldwide due to its unique advantages such as clean and safe, huge reserves and potential economic value [3-4].

With the continuous development of photovoltaic (PV) industry, the technology is becoming more and more mature, and the strong support of relevant government policies, the PV power generation industry has achieved tremendous development, and the cost of PV power plant construction has been greatly reduced compared with the previous years, but there is still room for decline [5-7]. In the actual photovoltaic project construction process, if the selected photovoltaic power plant construction address, then the capacity of the photovoltaic power plant and the total amount of each device is also basically determined, and the location of the convergence box, inverter, boosting station in the case of meeting the safe and stable operation of the system, there can be countless kinds of choice options, different options for the various levels of the convergence process of the cable use of varying degrees of impact [8-11]. Moreover, according to the design experience of engineering practice, the cost of high-voltage and low-voltage cables in photovoltaic power plants accounts for about 6% of the total cost, of which DC cables account for the main part, so in order to build highly efficient and economical photovoltaic power plants, it is necessary to plan and design the location of convergence boxes and inverters, so as to reduce the impact of the cable usage of photovoltaic power plants on the project cost, and to reduce the amount of cables can also effectively reduce the line power loss and improve the power generation efficiency of photovoltaic power stations [12-15]. At present, in the actual construction of photovoltaic power plants, there is no clear guideline for the design of multilevel converging cable connections, and the division of each converging zone in a photovoltaic power plant is still mainly dependent on the design experience of engineers and manual calculations, and lack of strict design optimization [16-18].

On the other hand, the current basis for cable selection is mainly along the traditional power grid generation, transmission and distribution network related design specification manuals, the current delivered by cables in the traditional grid is directly related to the nominal power of the system, while the current and system output power in the power generation characteristics of the PV power plant has a large efficiency loss relative to the installed capacity [19-21]. National and industry norms and standards point out the impact of system efficiency on the selection of cables for photovoltaic power plants, but do not specify the specific impact parameters [22-23]. At present, the selection of cables in the PV power plant design industry still follows the traditional selection parameters and standards, resulting in a certain amount of waste [24-25]. Therefore, it is of great application significance to refine the impact coefficient of power plant conversion efficiency by combining the actual construction experience [26-27].

This paper focuses on the optimization study of cable wiring scheme for photovoltaic power stations, highlighting the realistic need to optimize the cable wiring scheme by exploring the conventional cable wiring scheme and the problems existing in the wiring process. Taking power minimization as the objective function, the mathematical model of the cable wiring optimization problem is constructed under the constraints of current calculation, connectivity, branch current and node voltage. Aiming at the problem that the taboo search algorithm is difficult to find the optimal solution in large-scale problems, the initialization phase of the taboo search algorithm is improved by using the wild dog optimization algorithm. At the same time, the Lévy flight algorithm is used to perturb the suboptimal solution obtained by the wild dog optimization algorithm in each round of iteration, so as to solve the problem that the wild dog optimization algorithm is easy to fall into the local optimum. Through the improved taboo search algorithm on the construction of the wiring optimization model to solve, so as to explore the optimal cable wiring program in line with the model objectives and the economic benefits of photovoltaic power plant operation. A photovoltaic power plant is selected as the case study object of this paper, and the effectiveness and reasonableness of the improved taboo search algorithm is demonstrated by comparing the success rate of the improved taboo search algorithm with that of SaDE, CoDE and other algorithms in the process of model solving. Establish a test bench and build a simulation environment, and compare the alignment trends of the simulated cabling patterns obtained from this paper's optimization model with those of the actual patterns under the working conditions of obstacle avoidance, crossing holes, and narrowing channels, to explore the accuracy of this paper's optimization model. Finally, by comparing the wiring results obtained from this cable wiring optimization scheme and the original wiring scheme, the feasibility of the wiring optimization model based on the improved TS algorithm is highlighted in practical applications.

2. Analysis of cable wiring problems in photovoltaic power stations

2.1. Basic Structure of Photovoltaic Power Plants

Photovoltaic power stations can utilize relevant equipment or components to directly convert solar energy into electricity, and the photovoltaic power station units are more adaptable to the surrounding environment and can be directly set up in the distribution grid of the surrounding users. Generally speaking, the components in PV power stations, such as battery panels, control switches, energy storage batteries and capacitor adapters, are made of special materials. When generating electricity, the charging device tracks the maximum power point and transmits the electricity converted from solar energy on the battery panels to the energy storage batteries connected to the capacitor adapters, realizing the automatic regulation of capacitance. The construction of photovoltaic power plants between the distribution grid and the energy network, with appropriate optimization and adjustment, allows for the proper complement of the power dispatch between the two parties, ultimately integrating all the load profiles of the users, while the excess power is able to be transported to the public area for storage.

Because of the low operating costs, the construction of PV power plants has no size limitations or requirements, and the construction standards are highly flexible, but there are clear regulations on the performance of the accessories or components used in the construction process. Construction of photovoltaic power plants requires a large upfront cost, researchers need to continue to study the construction of photovoltaic power plants related to technology, through the optimization of the structure of the power plant or innovative components, to promote the development of the civilianization of photovoltaic power plant power generation mode.

2.2. Cable Wiring Methods for Photovoltaic Power Plants

2.2.1. Specialized cables for photovoltaics. The PV special cables on each module in the PV power station are led out from the positive and negative ports of each module, and laid to the ground through the back of the module bracket, and finally laid to the corresponding convergence box through the buried PVC protection pipe.

2.2.2. 1kV DC power cables. There are two places in the photovoltaic power station where 1kV DC power cables need to be laid, namely, the convergence box to the DC distribution cabinet and the DC distribution cabinet to the inverter. Due to the different wiring environments, the cable wiring forms in these two places are also different. The cable from the converter box to the DC distribution cabinet is directly buried in the field, and after the cable exits from the lower port of the converter box, it is directly buried along the open space at the edge of the components in the field to the DC distribution cabinet in the inverter room.

The cables from the DC distribution cabinet to the inverter section are laid in the cable trench inside the inverter room, and the cables come out from the lower port of the DC distribution cabinet, and are laid along the brackets in the indoor cable trench to the corresponding inverters.

2.2.3. 1kV AC power cables. After the DC power is converted into AC power by the inverter, a 1kV AC cable needs to be laid to the local box transformer. This section of cable from the inverter outlet, through the indoor cable trench, leading to the neighboring box-variable room of the buried pipe laid to the box-variable room in the box-variable. In order to meet the requirements of transmission capacity and wiring conditions, this section of the cable is generally laid in the form of multiple collocation.

2.2.4. 35kV AC power cables. 35kV AC power cable as the field collector line will be sent out of the box substation power to the field switching station or booster station, generally from the box substation high-voltage side of the cable room to the outgoing line, will be connected to the nearest box substation is completed, and ultimately to a larger cross-section of one or more cables laid to the station in the corresponding feeder switchgear.

2.3. Common Problems of Cable Wiring in Photovoltaic Power Plants

2.3.1. Problem of blindness. In the photovoltaic power station cable wiring, blindness problem is more common, its main performance is in the field cable wiring construction process, not get the effective guidance of the construction drawings, or there is no particularly standard and reliable construction drawings, the construction staff work relatively more random, especially in the classification of cables and the overall control of the direction of the problem of blindness is not to be ignored. For some photovoltaic power station cable wiring construction personnel, it is often believed that as long as there is a cable inventory, or has a cable, bracket and equipment related to the layout of the map, will be able to better complete the cable wiring task, so that in the subsequent cable wiring is often mixed with more of their own understandings and decisions, and then it is difficult to form an accurate wiring effect, there will be a significant deviation from the original construction intentions. In addition, if the cable wiring construction personnel are not able to accurately grasp the true intentions of the design drawings want to express, do not get the effective guidance of the designers, also prone to blindness of the wiring problem.

2.3.2. Problems of arbitrariness. Current PV power station cable wiring construction there is also a more obvious problem of arbitrariness, especially for some do not have a high cable wiring qualification staff, it is easier to be more casual in the wiring processing, only consider the convenience of their own construction operations, ignoring the relevant wiring standard requirements, or did not take into account the neatness and aesthetics of the requirements, resulting in the cable wiring results in the lack of reasonable. Part of the cable wiring construction personnel tend to think that as long as the cable is reasonably arranged to the required location, to ensure that the connection can be more accurate and solid, will be able to better protect the subsequent photovoltaic power station corresponding power electrical system stable operation, and then for the length of the cable as well as the winding method of insufficient attention, showing the obvious arbitrariness of the problem, so there will be, not only affects the cable aesthetics, but also may be the heat dissipation Problems such as improper, threatening its long-term stable operation.

2.3.3. Problems of incoherence. In the photovoltaic power station cable wiring construction, because of the lack of coordination of the problems brought about by the same can not be ignored, especially in the face of the current stage of the increasingly complex cable layout tasks, it is more likely to appear some of the conflicting issues, in the extension of the duration of the same time, will also bring some serious quality hazards. For some large-scale construction of photovoltaic power plant construction, cable wiring work often involves a number of subcontractors, these subcontractors if the lack of sufficient in-depth communication and coordination, is bound to lead to the implementation of their respective tasks in the lack of a global view, did not have the ability to take into account the associated subcontractor task requirements, not only increases the other cable wiring processing difficulties, the need for adjustment, often also Easy to increase the construction quality impact factors, resulting in the overall cable routing is not coordinated. Of course, this uncoordinated cable wiring construction will also directly lead to the final photovoltaic power plant cable wiring is relatively disorganized, can not be unified for all subcontractors constraints and requirements, increasing the difficulty of the subsequent maintenance management, but also increase the subsequent occurrence of the chances of security risks.

3. Cable routing optimization model based on TS algorithm

According to the research on the current commonly used cable wiring methods in PV power stations and their existing problems, this section will construct a cable wiring optimization model for PV power stations based on the taboo search (TS) algorithm. Firstly, the mathematical problem of PV power station cable wiring optimization is established, and the objective function and constraints of cable wiring optimization are studied. Secondly, the principle and process of the taboo search algorithm are briefly introduced, and the problems existing in the original taboo search algorithm are improved. Finally, an optimization model is established based on the improved taboo search algorithm to optimize and improve the cable wiring scheme of the photovoltaic power plant, so as to achieve the purpose of reducing the power supply loss of the line and improving the economic performance of the photovoltaic power plant operation.

3.1. Mathematical model of the cable routing optimization problem

3.1.1. Objective function. The main objective functions used for cable wiring optimization in PV power plants are: reducing power loss in the line network, reducing power loss, voltage quality, number of switching actions and balancing the loads between cable lines [28].

Optimization of cable wiring can reduce power losses, eliminate overloads, balance loads, and improve the quality of supply voltage. The power loss discussed in the usual sense of cable wiring optimization refers to the active loss generated on the operating line, in order to improve the economic performance of PV power plant operation, this paper optimizes the active loss during the operation of the cable line of PV power plant, i.e., to minimize the active loss of the whole network as the objective function, and its specific mathematical expression is:

$$\min P_{Loss} = \sum_{i=1}^{N_b} K_i \times R_i \times \frac{P_i^2 + Q_i^2}{U_i^2} \tag{1}$$

where N_b represents the total number of branches in the network. K_i is the state of the switch i, with 0 and 1 representing the disconnected and closed states of the switch, respectively. P_i, Q_i represents the active and reactive power flowing through branch b_i, respectively. R_i and U_i represent the branch resistance of branch b_i and its terminal node voltage, respectively.

3.1.2. Constraints. Since the operation of PV power plants must meet the conditions of closed design and open operation, the following constraints must be considered in the cable routing optimization process:

1) Tidal flow constraints, i.e:

$$P_i = P_{Di} + U_i \sum_{j=1}^{N_b} U_j (G_{ij} \cos\delta_{ij} + B_{ij} \sin\theta_{ij})$$
$$Q_i = Q_{Di} + U_i \sum_{j=1}^{N_b} U_j (G_{ij} \sin\delta_{ij} + B_{ij} \cos\theta_{ij}) \quad (2)$$

where $P_i, Q_i, P_{Di}, Q_{Di}, Q_{Di}, Q_{Di}$ denotes the active and reactive power of the load at node i and node i, respectively. $U_i, U_j, G_{ij}, B_{ij}, \delta_{ij}$ and θ_i denote the voltage, conductance, and conductance, as well as the conductance phase angle difference and the conductance phase angle difference at node i and node j, respectively.

2) Connectivity constraint, i.e., the cables of the PV plant must ensure that power is supplied to each load node during normal operation, i.e., there are no power supply islands in the cable network.

3) Branch current constraints, the branch current constraints, that is, the constraints on the capacity of each cable line, the current flowing on each branch in the cable line network must not exceed the maximum current permitted for that line, that is:

$$I_i < I_{i,\max} \quad (3)$$

where I_i and $I_{i,\max}$ represent the actual current flowing through branch b_i and the maximum value of its allowable flow current, respectively.

4) Nodal voltage constraints, the voltage at each load node in the cable line network must be within the rated range, i.e:

$$U_{i,\min} < U_i < U_{i,\max} \quad (4)$$

where $U_i, U_{i,min}$ and $U_{i,\max}$ represent the actual voltage at node i and the maximum value of voltage allowed at that point, respectively.

3.2. Taboo Search Algorithm

3.2.1. Algorithm overview. Taboo search algorithm (TS) is a typical stochastic search algorithm [29], which is able to effectively avoid local optimum by further expanding the local neighborhood search and after global step-by-step exclusion. The three basic elements of the taboo search algorithm are the release criterion, the taboo table and the move, the top priority of the search is the taboo table, and the move element determines the efficiency and success rate of the search, and once there is an error in the move, it may not be able to send the correct criterion for the release of the taboo table, and the advantage of this algorithm lies in the fact that the entire taboo operation is separate, and the starting point of its operation is the feasible solution scheme, and then it is clear from where to start the search, so that the objective function values can be optimized to be able to move, thus overcoming the problem of falling into a local optimum. The taboo search algorithm selects and records the optimization process by means of a taboo table, and then starts the next operation, and so on until the final optimal solution is reached.

3.2.2. Key parameters. By setting the taboo table to be able to record the TS algorithm has been completed by the various operations, in order to achieve iterative optimization, and in this process will strictly follow the defiance of the guidelines may lift the individual ideal state of the prohibited operations, the current termination criteria, the fitness value function, the forbidden object, the length of the taboo, the candidate solution, the defiance of the guidelines, the field function are the key parameters of the TS algorithm, the specific content of each parameter is as follows:

1) Fitness value function. The fitness value function in the TS algorithm can be any objective function, which is evaluated by searching the state and filtering the new current solution according to the contempt criterion and taboo criterion.

2) Taboo Object. Taboo table has been in a state of change in the elements are included, the meaning of taboo is to prevent the search into the local, thus affecting the speed of the solution, usually the target value, or the history of access to the state, the point can be a taboo object, if the representation of the criterion can be ignored for the time being, then iterative taboo object preference by the first-in-first-out way to achieve.

3) Taboo length. The maximum number of times a taboo object is not allowed to be selected without considering the defiance criterion is the size of the taboo table, also known as the taboo length, which can be fixed or variable.The search speed and the quality of the optimal solution of the TS algorithm largely depend on the taboo length, so it is one of the key parameters of the algorithm.

4) Candidate solutions. If a large number of neighborhood solutions are available, continuous attempts are required to improve the computational efficiency.

5) Contempt criterion. In order to maintain the good state solution and further optimize the performance of the algorithm, then the search should be concentrated in the nearby domain of the good state.

6) Neighborhood function. A guiding principle for deriving new solutions. Under different neighborhood functions, the number of neighboring solutions varies from each other, and this will also have an impact on the search efficiency and the quality of the resulting solutions, so this function is also a key parameter of the taboo search algorithm.

7) Termination Criteria. At present, there are three criteria that are usually used to terminate the program search, and these criteria can avoid the time performance of the TS algorithm from being affected: first, the system will automatically stop the search when the target taboo frequency or function reaches a certain value and then no longer changes. Second, the maximum number of iteration steps criterion. Third, the system stops searching when the optimal configuration of the program does not match the lower bound of the problem, which is the fitness value deviation degree criterion.

3.2.3. Algorithm flow. The flow of TS algorithm is shown in Fig. 1. Specifically, the main steps of the TS algorithm are as follows: the first step is to determine the initial solution and the neighborhood, based on which a certain number of candidate solutions are selected, and if the best candidate solution for the corresponding objective value of the solution is better than the optimal solution that currently exists, its forbidden characteristics can be ignored, and at the same time, the objects corresponding to the optimal candidate solution are entered into the forbidden table and the forbidden tenure of all the objects in the table is modified; if this cannot be done If this is not possible, it is necessary to reconstruct the current solution until a solution that meets this condition is found; then continue to enter such a solution into the taboo table, and also modify the tenure of the objects until the abort condition is reached, sometimes this process needs to be repeated several times.

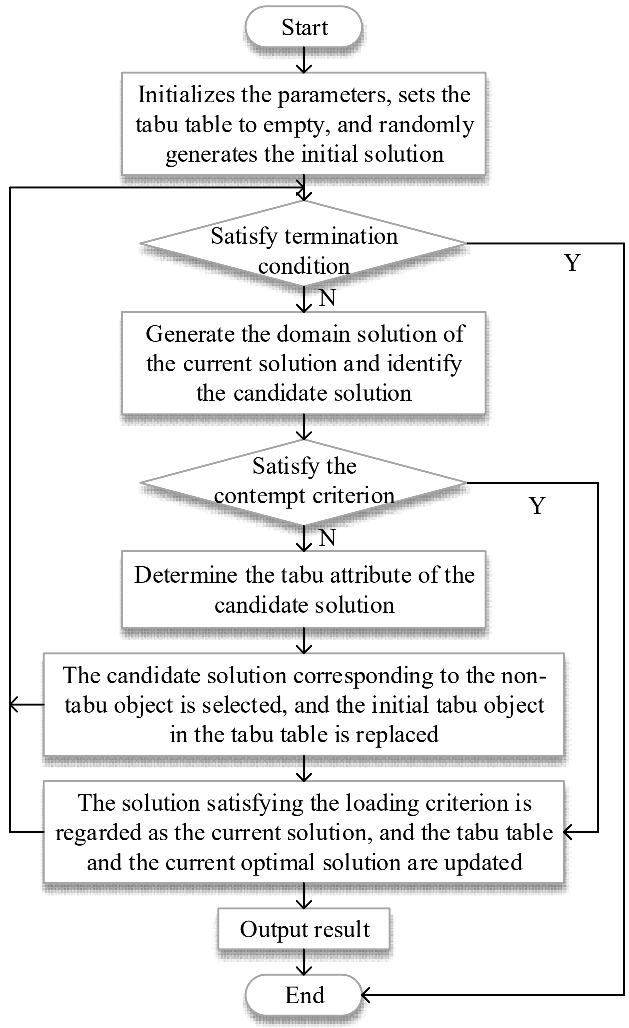

Fig. 1. Flowchart of Tabu search algorithm

3.3. Improvement of Forbidden Search Algorithm

Taboo search has the advantage of avoiding falling into local optimal solutions and preventing repetitive searches through a short-term memory system consisting of taboo tables. For low-dimensional problems, taboo search algorithms can yield good results. However, for large problems, the taboo search algorithm may be limited because it requires a large amount of resources to process the solution space. The initialization of the taboo search algorithm is generated in a random manner, and when the objective value is small relative to the data and the initial solution selected by simple random is very far away from the optimal solution, it is difficult to search for the optimal solution in the neighborhood of the feasible solution. The wild dog optimization algorithm has obvious competitiveness compared with other classical heuristic algorithms in a large number of benchmark test functions, and can most effectively achieve the global optimum with the smallest average absolute error, and can quickly converge in the initial stage of the iteration, and its iterative mechanism is very suitable for improving the defects on the forbidden search algorithm. Therefore, in this paper, the wild dog optimization algorithm is chosen to improve the initialization phase of the taboo search algorithm, in order to select a better initial feasible solution to improve the performance of the algorithm.

3.3.1. Wild Dog Optimization Algorithm. The Wild Dog Optimization Algorithm (DOA) is a group intelligence optimization algorithm inspired by the hunting strategy of wild dogs, which designs three strategies based on the social behaviors of wild dogs, which are group encirclement, individual attack, and scavenging behavior. Meanwhile, the survival probability strategy is added to this algorithm. The above multi-strategy form gives the DOA algorithm the advantage of fast convergence.The flow of DOA algorithm is shown in Fig. 2.

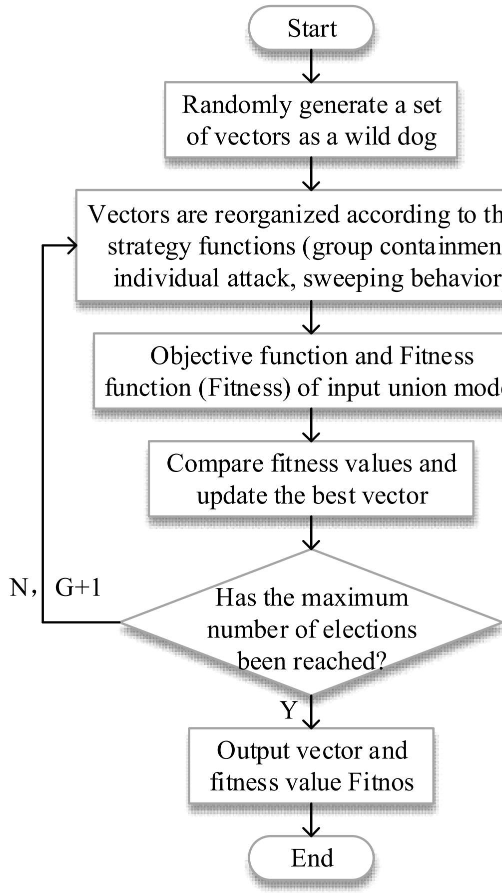

Fig. 2. Flow chart of Dingo optimization algorithm (DOA)

3.3.2. Improving the Wild Dog Optimization Algorithm Using Levy Flight. Since heuristic algorithms seek only to find a suboptimal solution, they usually adopt a greedy strategy or a local search strategy and simplify the problem to a certain extent so as to make the problem more manageable, which leads to the tendency to fall into a local optimum as a common problem that is difficult to avoid for most heuristic algorithms. In particular, algorithms with faster convergence speeds may converge to a local optimum solution prematurely. Therefore, even if DOA has a significant advantage over other heuristic algorithms in terms of efficiency, there still exists the possibility of not reaching the global optimum.

The Lévy flight algorithm [30], which is related to chaos theory, varies on the random step size and adopts a way of interspersing a short search and a long walk, and there exists a relatively large chance of a large stride during the random walk, which helps the algorithm's locally optimal solution to escape. Therefore, in this paper, we use the Lévy flight to carry out perturbation operations on the suboptimal solution obtained by each round of iteration of the DOA algorithm to prevent it from falling into the local optimum.

The trajectory of the Lévy flight is modeled by equation (5):

$$x_i'(t) = x_i(t) + l \oplus Levy(\lambda) \tag{5}$$

where $x_i(t)$ represents the i rd solution of generation t. l is the weight of the control step. $\oplus$ is the dot product. $Levy(\lambda)$ represents the path obeying the Lévy distribution. Due to the complexity of the Lévy stabilizing distribution, the Mantegna algorithm is mainly used to simulate it, and the step size is calculated from equation (6):

$$s = \frac{\mu}{|v|^{1/\gamma}} \tag{6}$$

where μ and v follow a normal distribution; γ is a constant factor that usually takes the value of 1.5.

The DOA algorithm has a significant advantage in convergence speed compared with other algorithms, and therefore the probability of falling into a local optimum is greater. The LDOA algorithm is obtained by improving the DOA algorithm using Lévy flight, and when the maximum number of iterations is not reached and the change of the fitness value tends to level off, the current solution is optimized according to Eq. (5) using the Lévy flight strategy before the next round of iterations, which can prevent the algorithm from falling into the local optimum.

3.4. Optimized model solution

The main steps of applying the improved TS algorithm to solve the cable routing optimization problem for PV power plants are as follows:

1) Read in the original data. Including network parameters, forbidden table depth, the maximum number of iterations $K_{\max}$ and the number of test solutions generated by each get band $S_{\max}$ and so on.

2) Produce the initial solution R^0, this paper is the original structure of the cable network. Set the current solution $R^C = R^0$, the optimal solution $R^{opt} = R^0$.

3) Produces a test solution. The inter-switching move t_{ij} acts on the current solution to produce a trial solution. i by randomly determining it in the set of open switches and j by randomly selecting it in the ring formed by closed switches i. The corresponding current and objective function values are calculated and the test solution is regenerated if any line capacity or node voltage is out of limits. Repeat this step until the number of test solutions reaches the required number $S_{\max}$.

4) Update the current solution. Select the solution with the optimal objective value among the test solutions R^*, and update the current solution with the movement that generated the solution if it is not in the taboo table or if it is in the taboo table but has already reached the release level R^C. If the movement that generated the solution is in the taboo table but has not reached the release level, select the suboptimal solution and repeat the process.

5) Update the taboo table. Store the reverse move of the realized move in the taboo table.

6) Update the optimal solution. If the objective value of the new current solution is less than the objective value of the optimal solution, update the optimal solution with the new current solution.

7) If the number of iterations does not reach $K_{\max}$, turn to step 3), otherwise end.

4. Case studies and simulation experiments

4.1. Case Selection

Photovoltaic power station is generally 1MWp photovoltaic array for a power generation unit configured with a group of inverters, so this paper takes 1MWp 11*8 photovoltaic array as an example for the cable routing and convergence box and inverter location optimization, which is configured with an inverter room, which is equipped with two sets of 500kW inverters. PV panels have two types of vertical and horizontal arrangement, in the case of the same footprint, the vertical arrangement is more than the horizontal arrangement to save the amount of cable, so this paper adopts the vertical two rows of the arrangement. PV panels to the convergence box between the PFG1169-1 × 4 photovoltaic cable, convergence box to the inverter between the use of ZRC-YJV22-0.6/1Kv-2 × 70mm2 power cables, the use of 16 into 1 out of the DC convergence box.

4.2. Performance analysis of improved TS algorithm

In order to verify the performance of the forbidden search algorithm (LDOA-TS) improved by using the improved wild dog optimization algorithm in this paper, SaDE and CoDE algorithms are selected for comparative analysis. In the experiment, 10 typical standard test functions are used for testing, and Table 1 shows the name, mathematical expression, search range and global optimal solution of each test function. Among them, function $f_1 - f_4$ is a unimodal function and $f_5 - f_{10}$ is a multimodal function.

Table 1. 10 standard test functions

Function name	Mathematical expression	Search range	Global optimal value
Sphere	$f_1(x)=\sum_{i=1}^{N} x_i^2$	[-150,150]	0
Schwefel 2.22	$f_2(x)=\sum_{i=1}^{N} \vert x_i \vert + \prod_{i=1}^{N} \vert x_i \vert$	[-20,20]	0
Zakharov	$f3(x)=\sum_{i=1}^{N} x_i^2 + (\sum_{i=1}^{N} 0.5ix_i)^2 + (\sum_{i=1}^{N} 0.5ix_i)^4$	[-10,10]	0
Rosenbrock	$f_4(x)=\sum_{i=1}^{N-1} (100(x_{i+1}-x_i^2))^2 + ((x_{i-1})^2)$	[-3,3]	0
Griewank	$f_5(x)=1+\frac{1}{4000}\sum_{i=1}^{N} x_i^2 - \prod_{i=1}^{N} \cos(\frac{x_i}{\sqrt{i}})$	[-500,500]	0
Schaffer 2	$f_6(x)=\sum_{i=1}^{N-1} (x_i^2 + x_{i+1}^2)^{0.25} (\sin^2(50(x_i^2+x_{i+1}^2)^{0.1})+1)$	[-50,50]	0
Schwefel 2.26	$f_7(x)=-\sum_{i=1}^{N} (x_i \sin(\sqrt{\vert x_i \vert}))$	[-300,300]	-423.754N
Himmelblau	$f_8(x)=\frac{1}{N}\sum_{i=1}^{N} (x_i^4 - 16x_i^2 + 5x_i)$	[-100,100]	-78.486
Ackley	$f_9(x)=-20\exp(-0.2\sqrt{\frac{1}{N}\sum_{i=1}^{N} x_i^2}) - \exp(\frac{1}{N}\sum_{i=1}^{N}\cos(2\pi x_i)) + 20 + e$	[-35,35]	0
Rastrigin	$f_{10}(x)=10N+\sum_{i=1}^{N} (x_i^2 - 10\cos(2\pi x_i))$	[-10,10]	0

In order to verify the convergence speed and reliability of the LDOA-TS algorithm, two indexes, the function evaluation times (FES) and the success rate (SR), are selected for measurement.FES is the average value of the number of target function evaluations required for the algorithm to reach a given accuracy $\delta = 0.0001$ within a set number of target function evaluations of 100,000 times for the error $(f(x) - f(x^*))$ of the function value, where $f(x)$ is the optimal value required by the algorithm and $f(x^*)$ is the global SR is the ratio of the number of successful solutions of the algorithm to the total number of runs, where it is specified that the algorithm is successful when it achieves the given accuracy $\delta = 0.0001$ within 100000 function evaluations.

Table 2 shows the number of function evaluations FES and the success rate SR for each algorithm, where "NA" means that the optimal function value obtained by the algorithm within the set number of target function evaluations of 100,000 times fails to achieve the given accuracy δ. It can be seen from the table that, for the majority of the functions, the convergence speed of the LDOA-TS algorithm is better than that of the SaDE algorithm and CoDE algorithm. Specifically, in terms of FES, the SaDE algorithm outperforms the LDOA-TS algorithm only on f_2 and f_6, and CoDE does not outperform the LDOA-TS algorithm on any function. In terms of SR, the SaDE algorithm solves 100% successfully for only 3 functions, the CoDE algorithm can solve 100% successfully for 5 functions, and the LDOA-TS can solve 100% successfully for all functions. Secondly, the average value of the last row in the table shows that the LDOA-TS algorithm requires the least number of objective function evaluations, which is 41,791, and the SaDE algorithm and CoDE algorithm are 79465 and 94764 respectively, i.e., the LDOA-TS algorithm saves 47.41% and 55.90% of the number of objective function evaluations with respect to the SaDE and the CoDE respectively, and Since the LDOA-TS algorithm makes the algorithm jump out of the local optimum by utilizing the TS algorithm's taboo on the local optimum, it has the highest reliability, with an average success rate of 1.000, compared to 0.818 and 0.972 for SaDE and CoDE algorithms, respectively.

Table 2. Function evaluation number and success rate

Function	N	SaDE		CoDE		LDOA-TS	
		FES	SR	FES	SR	FES	SR
f_1	50	21863	0.78	42135	1.00	**17463**	1.00
f_2	50	**24329**	0.84	57864	0.96	27439	1.00
f_3	50	147859	0.92	78943	1.00	**58421**	1.00
f_4	50	NA	0.00	239747	1.00	**102683**	1.00
f_5	50	22531	0.71	45831	0.97	**15326**	1.00
f_6	50	**70864**	1.00	196208	0.93	73482	1.00
f_7	50	39782	1.00	60359	1.00	**30473**	1.00
f_8	50	23481	0.95	37462	1.00	**18739**	1.00
f_9	50	32458	1.00	57604	0.95	**21574**	1.00
f_{10}	50	63974	0.98	131483	0.91	**52308**	1.00
Mean		79465	0.818	94764	0.972	41791	1.000

Two metrics, the mean function error value (ME) and the standard deviation value (Std), were chosen to measure the performance of each algorithm on the results obtained from the 10 test functions. In addition, in order to verify whether the proposed improved algorithm has a significant advantage over other algorithms, the Wilcoxon Signed Rank Test was selected to test the non-parametric hypothesis of the results obtained by 50 optimizations of each algorithm, and the significance level was 5%, with "+" indicating that the proposed algorithm was significantly better than the compared algorithm, "-" indicating that the proposed algorithm was significantly worse than the compared algorithm, and "≈" indicating that there was no significant difference between the two algorithms.

Table 3 shows the performance data of the algorithms for the results obtained by solving each test function in 50 dimensions, and the statistical results of the Wilcoxon Signed Rank Test nonparametric test in the last row of the table. From the data in the table, it can be seen that the LDOA-TS algorithm outperforms the SaDE algorithm and the CoDE algorithm for most of the results obtained by solving the functions. Specifically, the LDOA-TS algorithm significantly outperforms the SaDE algorithm for seven functions, including three unimodal functions (f_1, f_2, f_4) and four multimodal functions (f_5, f_6, f_8, f_{10}), while the SaDE algorithm significantly outperforms the LDOA-TS algorithm for only one function, and for the rest of the functions, since both the LDOA-TS algorithm and SaDE algorithm find the globally optimal solution and thus obtain the same The CoDE algorithm did not significantly outperform the LDOA-TS algorithm for any function and obtained the same result as the LDOA-TS algorithm for only 1 function (f_8), while the LDOA-TS algorithm significantly outperformed the CoDE algorithm for 9 functions.

Table 3. 50 dimensional optimization results of each function

Function	N	SaDE	CoDE	LDOA-TS
		ME(Std)	ME(Std)	ME(Std)
f_1	50	0.765(0.011)$^+$	0.841(0.048)$^+$	**0.554(0.015)**
f_2	50	0.869(0.035)$^+$	0.952(0.023)$^+$	**0.558(0.012)**
f_3	50	**0.574(0.010)**$^-$	0.867(0.047)$^+$	0.615(0.012)
f_4	50	0.885(0.019)$^+$	0.943(0.047)$^+$	**0.639(0.009)**
f_5	50	0.984(0.016)$^+$	0.848(0.023)$^+$	**0.663(0.011)**
f_6	50	0.773(0.037)$^+$	0.882(0.049)$^+$	**0.651(0.012)**
f_7	50	**0.541(0.024)**$^\approx$	0.938(0.042)$^+$	**0.541(0.024)**
f_8	50	0.743(0.031)$^+$	**0.732(0.034)**$^\approx$	**0.732(0.034)**
f_9	50	**0.763(0.036)**$^\approx$	0.897(0.0223)$^+$	**0.763(0.036)**
f_{10}	50	0.787(0.054)$^+$	0.852(0.018)$^+$	**0.537(0.017)**
+/≈/-		7/1/1	9/2/3	

From the above results and analysis, it can be seen that the LDOA-TS algorithm proposed in this paper outperforms the compared algorithms for solving most of the test functions, not only in terms of fast convergence speed and reliability, but also in terms of higher quality of solutions.

4.3. Wiring Optimization Model Simulation Experimental Analysis

4.3.1. Test stand design. In order to better verify the accuracy of the optimization models and algorithms in this paper, this paper builds a cabling test bed with the same working environment as the simulation and designs working conditions to compare and verify. The test bench takes the selected PV power plant as a prototype, and simulates the cable wiring pattern in multiple working conditions. Select a copper multi-core cable, model RVV, the implementation of the standard GB/T5023 5-2008, in order to facilitate the cable form into the capture, the need to select the adjacent points on the surface of the cable at intervals of 0.05m for marking. Cable end connectors choose M-type nylon waterproof cable connector, model M12 × 1.5, the connector consists of compression head, sealing ring, clamping claw and clamping nut. When in use, the sealing ring is put on the outer surface of the cable, the sealing ring is compressed by twisting the tightening head to fix one end of the cable in the clamping claw, and the other end of the connector is connected with the electrical components through the threaded nut. Cable wiring in addition to electrical components, connectors in addition to the design of obstacles. The obstacles in the cable wiring process are made using 3D printing. The selected profile is PLA material, which is inexpensive, odorless, has a good surface smoothness, and is suitable for printing large-size pieces.

4.3.2. Experimental results and analysis. According to the cabling conditions designed in the previous paper, this paper will compare and analyze the errors of single-condition morphology such as obstacle avoidance condition, over-hole condition, and over-narrow-channel condition, respectively. By designing the same conditions on the cable morphology test bench, the actual morphology of the cable is obtained, and the accuracy of the model is verified by comparing with the simulated morphology.

1) Obstacle avoidance condition. For the obstacles existing in the cable wiring process, in this section, two types of planar obstacle avoidance and spatial obstacle avoidance are designed for comparison with three groups of working conditions. The two ends of the cable are fixed on both sides of the test

bench through the cable connector, and the different working conditions are designed by changing the position of the connector on the wall of the test bench.

For the planar obstacle avoidance condition, only the morphology in the frontal camera plane is compared and analyzed due to the common surface at the beginning and end positions, and the results are shown in Fig. 3, with (a)-(c) indicating the comparison results between the actual morphology of the cables in the planar obstacle avoidance conditions 1, 2, and 3 and the simulation results, in units of cm, respectively, and the actual spatial morphology of the cables is obtained by importing the acquired morphology coordinates into the morphology solver and the fitting program. Comparing the actual spatial morphology with the optimized cable routing results, the simulation results of the optimized cable routing are similar to the actual morphology and the alignment trend is the same under the planar obstacle avoidance condition. It is proved that the optimization model proposed in this paper can calculate a reasonable static equilibrium shape of the cable for obstacle avoidance condition.

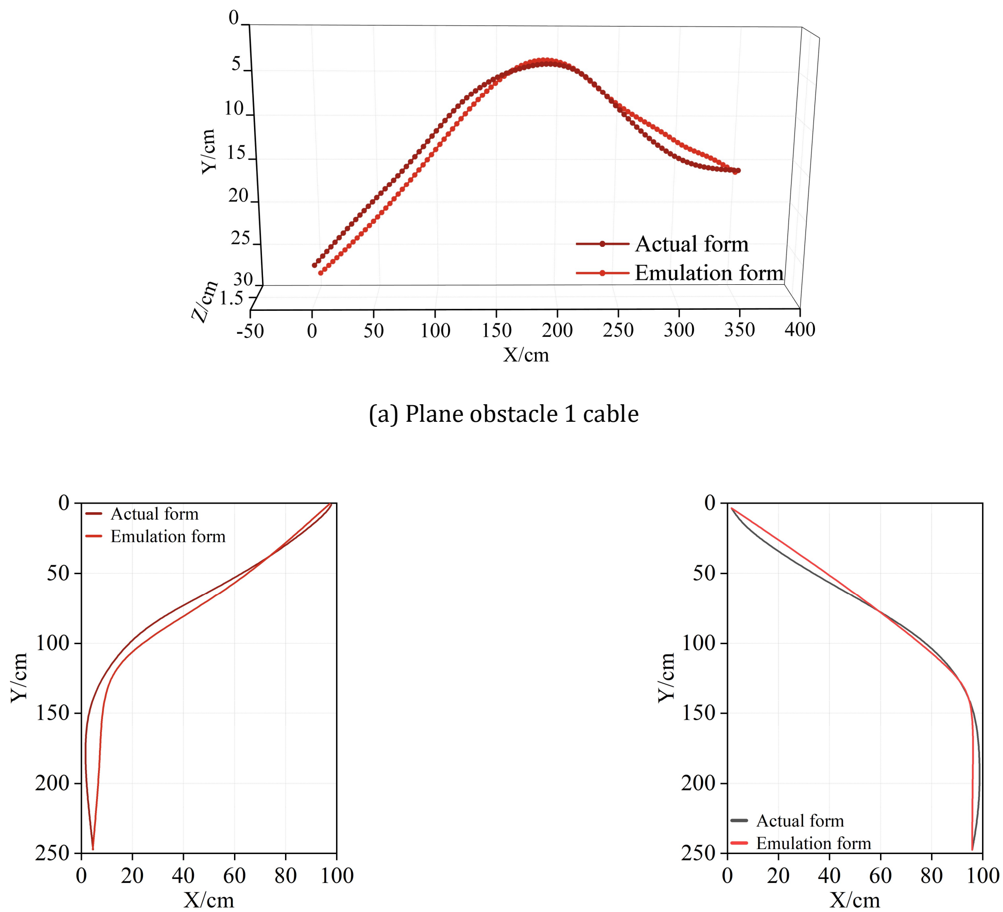

(a) Plane obstacle 1 cable

(b) Plane obstacle 2 cable

(c) Plane obstacle 3 cable

Fig. 3. Comparison of cable configuration in plane obstacle avoidance condition

For the spatial obstacle avoidance condition, the beginning and end of the cable are not known to be in the same plane, so it is necessary to compare and analyze its spatial morphology, and the results are shown in Fig. 4, and (a)-(c) represent the results of comparing the actual morphology of the cable with the simulated morphology of the spatial obstacle avoidance conditions 1, 2, and 3, respectively, with the unit of cm. for the morphology of the cable in the spatial obstacle avoidance condition, the cable actual morphology matches with the simulated morphology when the cable beginning and end position centerline directions are parallel. The actual morphology of the cable is consistent with the simulated morphology. When the centerline of the beginning and end positions are perpendicular, the actual shape of the cable has a larger error than the simulated shape. This is because in the initial path search process, the algorithm tends to select nodes that do not bend or have a smaller degree of bending. In the actual cable routing process, the cable has a large stiffness, the part near the initial end will remain close to the straight line of the form, and then bending occurs, so when the centerline of the beginning and end of the direction of the center line is perpendicular to the direction of the cable, it will lead to a larger error in the form. However, it can be seen that the simulation and the experiment have the same alignment trend, and the simulation form is smoother than the actual form. Therefore, the algorithm and model can get more accurate wiring results under obstacle avoidance conditions, which verifies the accuracy of the model and algorithm.

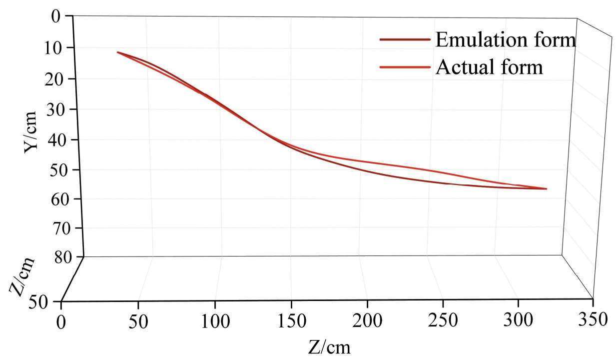

(a) Space obstacle 1 cable

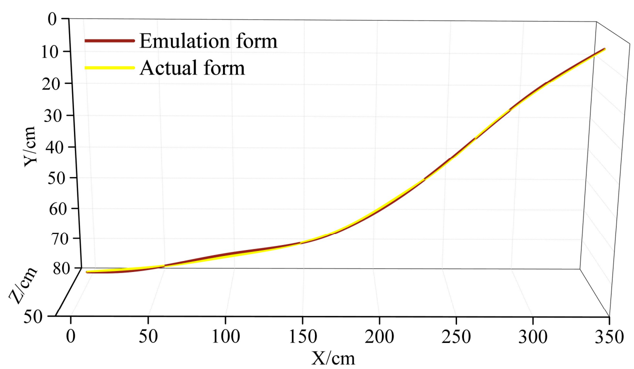

(b) Space obstacle 2 cable

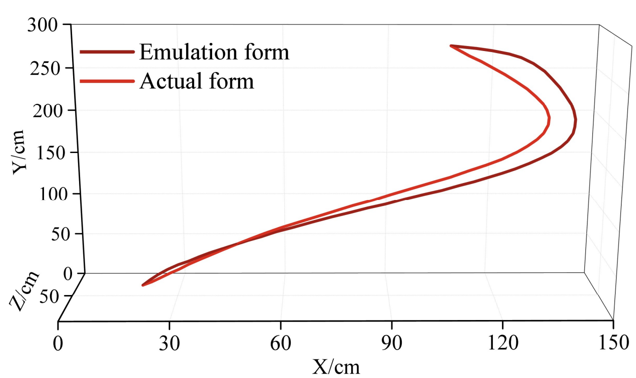

(c) Space obstacle 3 cable

Fig. 4. Comparison of cable configuration in space obstacle avoidance condition

2) Over-hole condition. In order to verify the accuracy of the cable wiring optimization model and experiments under extreme conditions, this paper carries out the wiring experiments with the same boundary conditions on the test bench according to the perforated condition of the photovoltaic power plant. The comparison between the actual and optimized cable routing in the hole crossing condition is shown in Fig. 5, (a)-(c) represent the comparison between the actual and simulated forms of the hole crossing conditions 1, 2 and 3, respectively, in unit of cm. The simulated form and the actual form overlap with the position of the hole crossing, which indicates that the cable spatial coordinates are the same during the hole crossing, and the forms of the cables before and after the hole crossing are not the same. This is because in the initial path calculation process, the LDOA-TS algorithm tends to select spatially coplanar nodes in the process of selecting path nodes. However, the alignment trends of the simulation results and the actual results are basically the same, indicating that the model and algorithm in this paper can still obtain accurate wiring results when dealing with the over-hole condition.

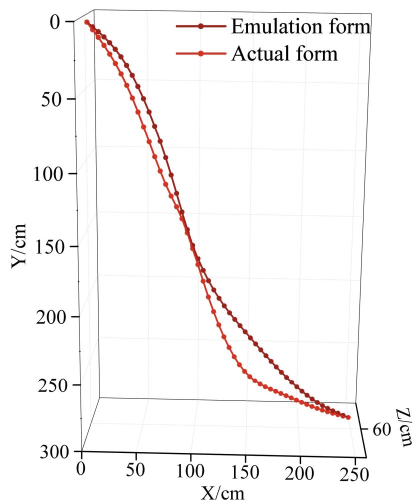

(a) Perforated condition 1

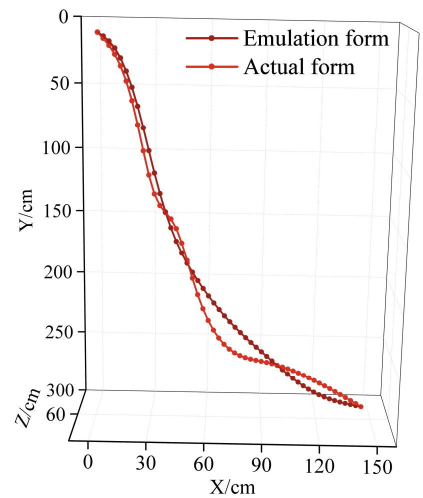

(b) Perforated condition 2

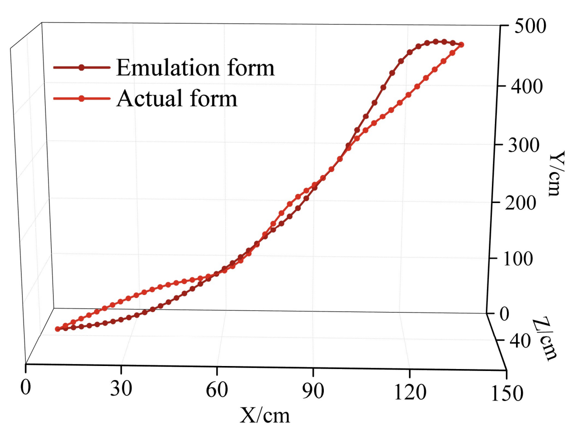

(c) Perforated condition 3

Fig. 5. Comparison of cable configuration under perforated conditions

3) Over-narrow channel condition. In order to verify the accuracy of this paper's method in the narrow channel condition, according to the narrow channel condition in the photovoltaic power plant, the wiring experiment with the same boundary conditions is carried out on the test bench. The comparison of the actual shape of the narrow channel condition and the optimized cable wiring results

is shown in Figure 6, and the unit is cm. The unit is cm. For the actual wiring results, the wiring results of cable optimized wiring are smoother. This is because in the actual project, the cables are placed in bundles before assembly, and there will be local bending in the wiring process. The simulation results in the figure have the same alignment trend as the actual results, which verifies the accuracy and feasibility of the model and algorithm proposed in this paper for the over-narrow channel condition.

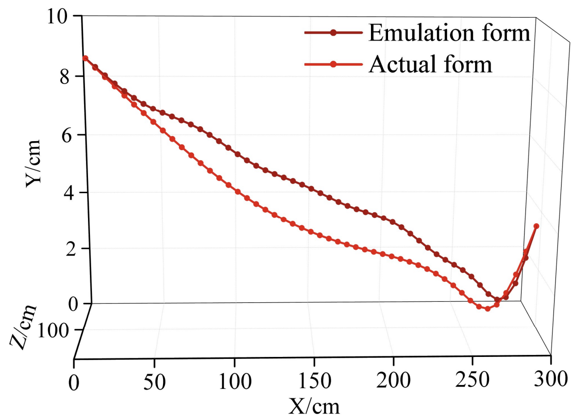

Fig. 6. Comparison of cable configuration under excessively narrow space condition

In order to verify the accuracy of the proposed method on the cable wiring length, this paper compares the length of the simulation form and the actual form, and the results are shown in Fig. 7, in which PL1-3 indicates the three conditions of planar obstacle avoidance, SP1-3 indicates the three conditions of spatial obstacle avoidance, PE1-3 indicates the over-hole conditions 1-3, and NA indicates the over-narrow-channel conditions, and the same below. From the figure, it can be seen that the cable morphology obtained according to the cabling optimization model under different working conditions compared with the actual morphology of the cable in the total length of the average error of 3.51%, the length difference of 150.05cm, the maximum error of a single root is 5.08%, the length of the error within 10%, to meet the requirements. In summary, it can be seen that the model and algorithm proposed in this paper are accurate in the calculation results for different working conditions, which verifies the accuracy and effectiveness of the model and algorithm.

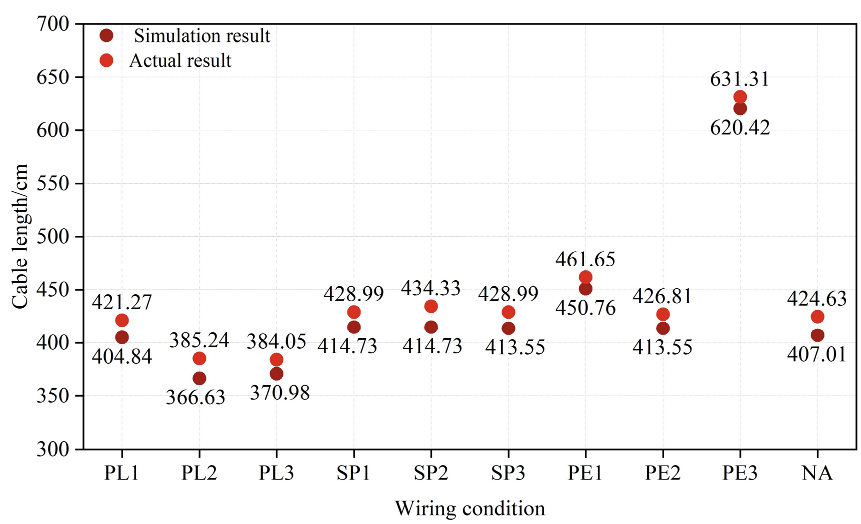

Fig. 7. Comparison between actual cable length and simulation length

4.3.3. Analysis of the effect of cable routing optimization. In order to further verify the effectiveness of the optimization model in this paper, the cable wiring diagrams in the two cases of considering the inverter position in the PV power plant with and fixed, the improved TS algorithm wiring is compared with the original wiring scheme. Fig. 8(a) shows the optimized cable wiring scheme for PV plant based on the improved TS algorithm when the inverter is random (Scheme I), and Fig. 8(b) shows the original conventional wiring scheme (Scheme II). The dark red part of the figure represents the location of the inverter, and the black part represents the location of the combiner box mounted on the PV bracket. From the figure, it can be seen that the original wiring scheme adopts parallel connection, and obvious power supply islands appear within the electric field of the PV plant. And Scheme 1 based on the improved TS algorithm adopts the combination of parallel and vertical connections to effectively avoid the problem of power supply islands and meets the connectivity constraints required by the optimization model in this paper.

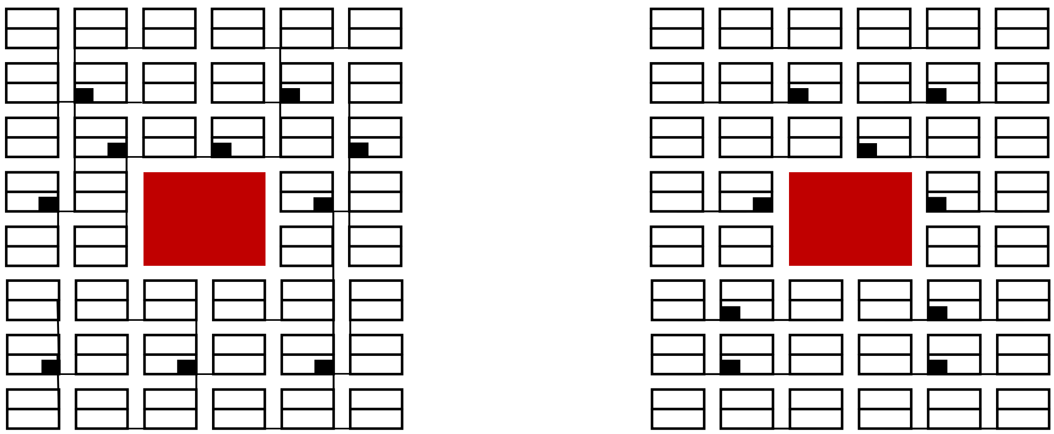

(a) Solution one (b) Solution two

Fig. 8. Wiring results of different schemes

Fifteen nodes are randomly selected in different design schemes to test the cable length of PV power plant and the power loss during cable operation, and the results are shown in Table 4. It is obvious from the data in the table that this paper achieves a significant optimization of PV power plant cable wiring using the improved TS algorithm. In terms of cable length, the cable length used in different nodes of cabling scheme I using the improved TS algorithm is smaller than that of the original cabling scheme II, and the average cable length used is 30.30% lower than that of scheme II. In terms of power loss, the power loss of scheme I at different nodes is also smaller than that of scheme II, and the average power loss is reduced by 49.95%. The experimental results show that the cable wiring optimization model of PV power plant designed based on the improved TS algorithm in this paper can successfully achieve the goal of power loss minimization under the constraints of current calculation. And compared to the original wiring scheme, the cable wiring scheme based on the improved TS algorithm will use a shorter cable line to achieve better results than the original wiring scheme, significantly highlighting the economic benefits of the program proposed in this paper, and more in line with the needs of the low-carbon era of photovoltaic power plant cable wiring.

Table 4. Comparison of wiring results of different schemes

Node number	Cable length(m)		Power loss(kW)	
	Solution one	Solution two	Solution one	Solution two
1	4071.04	5855.16	191.61	465.88
2	3103.28	6624.56	215.91	401.42
3	3334.07	5298.15	193.00	415.17
4	3841.46	6939.04	233.90	376.06
5	4975.02	6885.17	212.11	394.97
6	4615.95	6089.01	118.84	415.39
7	4953.23	6200.05	126.21	311.35
8	4538.28	5765.69	191.29	386.57
9	4201.45	5220.61	222.60	354.33
10	3532.65	6846.70	149.62	301.91
11	3484.86	5000.08	195.64	393.84
12	3673.79	5267.41	213.20	384.79
13	4727.88	5724.93	227.83	428.14
14	4112.11	5954.47	198.55	319.16
15	4926.39	5418.65	176.89	379.80
Mean	4139.43	5939.31	191.15	381.92

5. Conclusion

This paper establishes an optimization model of cable wiring scheme in photovoltaic power stations based on the taboo search algorithm, and improves it through the improved wild dog optimization algorithm to improve the possibility of obtaining the optimal solution of the model. A photovoltaic power plant is selected for case study and simulation experiments, and the following conclusions are successfully obtained:

1) The improved taboo search algorithm (LDOA-TS) in this paper has significant performance advantages over the SaDE algorithm and CoDE algorithm. The average number of function evaluations for LDOA-TS is 41,791 compared to 79,465 and 94,764 for SaDE and CoDE algorithms respectively, which is a decrease of 47.41% and 55.90% for LDOA-TS algorithm in comparison. Also the average solution success rate of LDOA-TS algorithm in 30-dimensional problems is 1.000, while the average success rate of SaDE algorithm and CoDE algorithm is 0.818 and 0.972, respectively. And in the Wilcoxon Signed Rank Test nonparametric test, the solution performance of LDOA-TS algorithm in most of the test functions is significantly optimized for the other two algorithms, which has the outstanding features of fast convergence speed, high reliability, and high quality of solution, indicating that the improvement of the forbidden search algorithm in this paper has a significant rationality.

2) Using the cable routing optimization model constructed in this paper to carry out simulation experiments, the morphology of the cable routing in different working conditions such as obstacle avoidance, crossing holes and narrow channels and the actual morphology are consistent with the trend of the alignment, and the difference between the two morphologies is small. This shows that the optimization model in this paper has high accuracy in cable routing morphology. Comparing the wiring scheme applying the wiring optimization model of this paper with the original wiring scheme, the results show that the wiring scheme of this paper can effectively connect all units in the PV power plant field and meet the connectivity constraints required by the optimization model of this paper. In addition, the average values of cable length and power loss required by the wiring scheme applying this paper's model are 4139.43 m and 191.15 kW, respectively, while the average values of the original scheme are 5939.31 m and 381.92 kW, respectively, which indicate that this paper's scheme can

effectively save cable wiring costs while meeting the optimization model's minimization of power loss, which shows obvious economic benefits, and provides a good solution for the construction and operation optimization of photovoltaic power plants in the low-carbon era. It provides an effective reference for the construction and operation optimization of photovoltaic power stations in the low-carbon era.

References

[1] He, X. H., Ding, H., Jing, H. Q., Wu, X. P., & Weng, X. J. (2021). Mechanical characteristics of a new type of cable-supported photovoltaic module system. Solar Energy, 226, 408-420.

[2] Wang, L., Yang, H., Zhang, X., Wei, K., Huo, Y., Xu, K., & Zhang, H. (2021, October). Research on Leakage Fault Mechanism of Photovoltaic Power Station Considering Photovoltaic Inverter. In 2021 9th International Conference on Smart Grid and Clean Energy Technologies (ICSGCE) (pp. 98-103). IEEE.

[3] Rebelo, R., Fialho, L., & Novais, M. H. (2024). Floating photovoltaic systems: photovoltaic cable submersion testing and potential impacts. Open Research Europe, 3, 61.

[4] Zhu, Y. F., Huang, Y., Guo, Y., Xiao, B., Chen, C. H., & Yao, Y. (2024). Numerical assessment of the initial pre-tension impact on wind-induced vibration in flexible cable-supported photovoltaic systems. Journal of Wind Engineering and Industrial Aerodynamics, 251, 105788.

[5] Lange, A., & Pasko, M. (2020). Selected aspects of photovoltaic power station operation in the power system. changes, 5, 6.

[6] Cabrera-Tobar, A., Bullich-Massagué, E., Aragüés-Peñalba, M., & Gomis-Bellmunt, O. (2016). Topologies for large scale photovoltaic power plants. Renewable and Sustainable Energy Reviews, 59, 309-319.

[7] Wang, L., Li, L., Fan, L., Nan, J., Xu, K., Huo, Y., ... & Chen, H. (2022, July). Research on the Insulation Detection Technology of the AC Cable in Distributed Photovoltaic Power Station Considering Photovoltaic Inverter. In 2022 2nd International Conference on Electrical Engineering and Mechatronics Technology (ICEEMT) (pp. 291-295). IEEE.

[8] Chakroun, R., Ayed, R. B., & Derbel, N. (2020). Combined SHE-LLCL design for a real case photovoltaic power station. Journal of Control, Automation and Electrical Systems, 31, 1558-1566.

[9] Gattuso, D., Greco, A., Marino, C., Nucara, A., Pietrafesa, M., & Scopelliti, F. (2016). Sustainable mobility: Environmental and economic analysis of a cable railway, powered by photovoltaic system. International Journal of Heat and Technology, 34(1), 7-14.

[10] Sahu, A., Yadav, N., & Sudhakar, K. (2016). Floating photovoltaic power plant: A review. Renewable and sustainable energy reviews, 66, 815-824.

[11] Atayev, S., Bayramova, G., Heydarova, L., & Mahizade, A. (2024, April). Industrial Design of Photovoltaic Power Station: Design Review. In International Conference on Smart Environment and Green Technologies (pp. 565-572). Cham: Springer Nature Switzerland.

[12] Malogulko Yuliia, V. (2022, May). DESIGN OF A 9.5 MW PHOTOVOLTAIC POWER PLANT. In The 10 th International scientific and practical conference "Science, innovations and education: problems and prospects"(May 4-6, 2022) CPN Publishing Group, Tokyo, Japan. 2022. 624 p. (p. 146).

[13] Chen, J., Xiong, K., Yan, W., Bao, Z., & Xu, S. (2023, July). Optimization of equipment layout and cable planning of photovoltaic power station based on genetic algorithm. In 2023 42nd Chinese Control Conference (CCC) (pp. 1-5). IEEE.

[14] Zhang, Y., Li, B., Du, Y., Ding, Y., Cao, J., & Lv, J. (2021). Effective grounding of the photovoltaic power plant protected by lightning rods. IEEE Transactions on Electromagnetic Compatibility, 63(4), 1128-1136.

[15] Yoo, B. J., Park, C. B., & Lee, J. (2016, November). A study on design of photovoltaic system using electrical railway stations. In 2016 19th International Conference on Electrical Machines and Systems (ICEMS) (pp. 1-5). IEEE.

[16] Ji, X., Fan, G., Liang, R., & Shi, J. (2024). Parallel Cable Mechanism Adjustment Strategy between Subsystems of Space Solar Power Station. International Journal of Automotive Manufacturing and Materials, 2-2.

[17] Buerhop-Lutz, C., Stroyuk, O., Pickel, T., Winkler, T., Hauch, J., & Peters, I. M. (2021). PV modules and their backsheets-A case study of a Multi-MW PV power station. Solar Energy Materials and Solar Cells, 231, 111295.

[18] Han, X. (2022). Photovoltaic Power Station Monitoring System Using GSM Wireless Communication Network. Academic Journal of Engineering and Technology Science, 5(1), 363-370.

[19] Klimenta, D., Jevtić, M., Andriukaitis, D., & Mijailović, V. (2021). Increasing the transmission performance of a conventional 110 kV cable line by combining a hydronic concrete pavement system with photovoltaic floor tiles. Electrical Engineering, 103(3), 1401-1415.

[20] Buerhop, C., Bommes, L., Schlipf, J., Pickel, T., Fladung, A., & Peters, I. M. (2022). Infrared imaging of photovoltaic modules: a review of the state of the art and future challenges facing gigawatt photovoltaic power stations. Progress in Energy, 4(4), 042010.

[21] Barbón, A., Bayón-Cueli, C., Bayón, L., & Carreira-Fontao, V. (2022). A methodology for an optimal design of ground-mounted photovoltaic power plants. Applied Energy, 314, 118881.

[22] Luo, Z., Qin, H., Cheng, T. E., Wu, Q., & Lim, A. (2021). A branch-and-price-and-cut algorithm for the cable-routing problem in solar power plants. INFORMS Journal on Computing, 33(2), 452-476.

[23] Mehta, S. (2022). SELECTIONS AND SIZING OF HT CABLE AND LT CABLE. “EV CHARGING STATION" May 2022, 108.

[24] Kozyra, J., Łukasik, Z., Kuśmińska-Fijałkowska, A., & Kaszuba, P. (2022). An analysis of remote voltage measurement in the medium voltage cable networks. Przegląd Elektrotechniczny, 98, 299-306.

[25] Cazacu, E., Groşanu, D. V., & Petrescu, L. (2021). Reactive power management in a grid-connected photovoltaic power station: a case-study. The Scientific Bulletin of Electrical Engineering Faculty, 21(2), 53-58.

[26] Goeritno, A., Maulana, M. A., Shulhan, F., & Fiqwananda, H. (2023). Pemasangan Solar Panel Untuk Sistem Charging Power Station di Kawasan Ekowisata Gunung Kuta, Kabupaten Bogor. Mitra Teras: Jurnal Terapan Pengabdian Masyarakat, 2(2), 82-97.

[27] Khan, F. U., Murtaza, A. F., Sher, H. A., Al-Haddad, K., & Mustafa, F. (2020). Cabling constraints in PV array architecture: Design, mathematical model and cost analysis. IEEE Access, 8, 182742-182754.

[28] Murilo Oliveira Machado,Islame Felipe da Costa Fernandes,Silvia Maria Diniz Monteiro Maia & Elizabeth Ferreira Gouvêa Goldbarg. (2024). A hybrid multi-agent metaheuristic for the offshore wind farm cable routing problem. Expert Systems With Applications(PC),124668-124668.

[29] El Bakali Saida,Ouadi Hamid,Giri Fouad,Gheouany Saad,Mounir Nada & Jrhilifa Ismael. (2024). Tabu Search Algorithm for Optimal Electric Water Heating Energy Management. IFAC PapersOnLine(13), 835-840.

[30] Babangida Modu,Md Pauzi Abdullah,Abdulrahman Alkassem & Mukhtar Fatihu Hamza. (2024). Optimal rule-based energy management and sizing of a grid-connected renewable energy microgrid with hybrid storage using Levy Flight Algorithm. Energy Nexus100333-100333.